Bruna B. Carvalho (bruna.borgescarvalho@unipd.it)

Revealing the link between A-type granites and hottest melts from residual metasedimentary crust

B.B. Carvalho[1,*], O. Bartoli[1], B. Cesare[1], M. Satish-Kumar[2], M. Petrelli[3], T. Kawakami[4], T. Hokada[5], M. Gilio[6]

[1] *Dipartimento di Geoscienze, Università di Padova, Via G. Gradenigo, 6. 35129, Padua, Italy.*

[2] *Faculty of Science, Niigata University, 8050 Ikarashi 2-no-chi, Nishi-ku, Niigata-shi 950-2181, Japan.*

[3] *Dipartimento di Fisica e Geologia, Università di Perugia, Piazza dell'Università 1, 06123, Perugia, Italy.*

[4] *Department of Geology and Mineralogy, Kyoto University, Kitashirakawa-Oiwake-cho, Sakyo-ku, Kyoto 606-8502, Japan.*

[5] *Geoscience Group, National Institute of Polar Research, 10-3 Midori-cho, Tachikawa, Tokyo, 190-8518, Japan.*

[6] *Dipartimento di Geologia, Università di Pavia, Via Adolfo Ferrata 1, 27100, Pavia, Italy.*

*corresponding author: bruna.borgescarvalho@unidp.it

ABSTRACT

Among S-, I-, and A-type granites, the latter are the most debated in terms of origin, and metasedimentary crust is usually discarded as potential source. Here we tackle this issue by adopting an in-source perspective, rather than focusing on the final product (granite), documenting the occurrence of pristine melt inclusions (MI) in garnet from residual metapelitic ultrahigh temperature (UHT) granulite from East Antarctica. Coexistence of sapphirine + quartz, phase equilibria calculations and Zr-in-rutile thermometry indicate that MI trapped UHT melts formed at peak conditions (930–1000 °C) from a residual metapelitic source. MI are granitic with weakly peraluminous to weakly peralkaline affinity, ferroan character, high alkali contents, high K/Na and Ga/Al, and low Ca, Ba, Sr, and H_2O concentrations. These features and geochemical modelling indicate that MI represent primary melts for high-SiO_2 A-type granites. Therefore, MI reveal the

missing link between A-type granites and the hottest metasedimentary crust. Voluminous amounts of slightly peraluminous, high-SiO_2 A-type granites can be produced in large, residual UHT terranes such as those of eastern Gondwana. Our results provide a wider view of processes responsible for granite formation and show that a larger variety of granites must be considered in models on the effects of UHT anatexis on crustal differentiation.

INTRODUCTION

A-type granites form at high temperature and show high $FeO_t/(FeO_t+MgO)$, high Ga/Al, high abundances of alkali, and high field strength elements, low CaO, H_2O, Ba, and Sr, ranging from metaluminous to slightly peraluminous, sometimes peralkaline (Collins et al., 1982; Whalen et al., 1987; King et al., 1997; Frost and Frost, 2011). Although less abundant than the classic S- and I-, the A-type granites occur in a variety of geodynamic contexts, including extraterrestrial materials (Bonin, 2007). Their origin is controversial and subject of debate (Collins et al., 2021; Eby, 1990; Creaser et al., 1991; Eby, 1992; King et al., 1997; Patiño-Douce, 1997; Huang et al., 2011; Frost and Frost, 2011). Petrogenetic models proposed for their formation are i) anatexis of (meta)tonalitic to granodioritic crust, ii) differentiation of basaltic melts, and iii) differentiation coupled with assimilation of crustal material (Collins et al., 1982; Eby, 1990; Frost and Frost, 2011). When felsic igneous protoliths are invoked as a source, the debate focuses on its possible residual (Collins et al., 1982; 2021) or fertile nature (Creaser et al., 1991; Patiño-Douce, 1997; Frost and Frost, 2011). Metasedimentary sources are not considered an option, despite some occurrences may indicate the contrary (Huang et al., 2011; Zhang et al., 2022).

Since the formation of A-type granites may require T >900 °C (Clemens et al., 1986; Collins et al., 2021), debating their crustal origin means entering the domain of ultrahigh temperature (UHT) metamorphism, where longer duration might be instrumental in generating larger volume of melts (Harley, 2016). Most studies on UHT granulites have focused on their strongly residual assemblages (Kelsey and Hand, 2015), whereas characterization of melts produced, and their impact on crustal differentiation remain poorly known (Clark et al., 2011).

Here we present new data on exceptionally preserved melt inclusions (MI) in garnet of granulites from Antarctica. We demonstrate that the MI formed at UHT conditions from a residual metapelitic source and that their melts share key geochemical features with many A-type granites. Our study provides the first in-source evidence linking high-SiO_2 A-type granites to the anatexis

of residual metasedimentary crust at UHT conditions.

GEOLOGICAL BACKGROUND AND RESIDUAL SOURCE ROCK

Metapelitic Mg-Al granulites occur as lenses within garnet-sillimanite and garnet-biotite gneisses at Rundvågshetta, Lützow-Holm Complex (East Antarctica) where a clockwise *P–T* path with peak *T* of 920–1040°C is well constrained (Durgalakshmi et al., 2021 and references therein). This UHT event, also recorded in Madagascar, Sri-Lanka and southern India, is related to continental collision and amalgamation of the Gondwana supercontinent at 550-520 Ma (Durgalakshmi et al., 2021; see Data Repository). As older (>600 Ma) high-grade metamorphic events are also recorded, the UHT metamorphism at Rundvågshetta has been interpreted to result from crustal pre-conditioning before Gondwana amalgamation (Durgalakshmi et al., 2021). The studied Mg-Al granulite is coarse-grained and layered, with predominant mafic domains and less abundant felsic ones (Fig. 1A, see Data Repository).

UHT CRUSTAL MELTS PRESERVED IN GRANULITIC GARNET

In the felsic domain (Fig. 1B) garnets contain clusters of inclusions with zonal arrangement, indicating entrapment during garnet growth (Cesare et al., 2015). Inclusions consist of quartz and accessory zircon, rutile and apatite, and both glassy, and crystallized MI (i.e., *nanogranitoid*; Cesare et al., 2015). The exceptionally preserved glassy inclusions (GI) are very small (5 to 25 μm) and contain isotropic glass (Fig. 1 C), whereas the coexisting nanogranitoids (NI) are larger (5-150 μm) and contain feldspars, quartz and biotite (Fig. 1D-F). Accidentally trapped phases in MI are apatite, rutile and occasionally touching sapphirine + quartz (hereafter Sa + Qz) (Fig. 1D-E). The Sa + Qz pair is also found as composite inclusions in MI-bearing garnet. As this sapphirine has low Fe^{3+}/Fe_{total} (0.11-0.25; Table DR1), the Sa + Qz association is a strong evidence that garnet in felsic domains grew at UHT.

A *P–T* phase diagram was calculated (Figure 2A; see Data Repository for modelling strategy), considering the path proposed by Durgalakshmi et al. (2021) for the last UHT event at Rundvågshetta (Fig. 2A). According to the calculations, garnet may grow in the stability field of Sa + Qz, melt and rutile (i.e., garnet can trap these phases) when following an isobaric cooling at ≈8 kbar. The model predicts that ≈12 vol.% melt is present at peak conditions (≈1040 °C and 8

kbar) and that ≈15 vol.% garnet can form by cooling down to 925°C, trapping inclusions of UHT melt (Fig. 2A).

Rutile is associated with MI in garnet (Fig. 1B-C) and coexists with zircon and quartz both in garnet and matrix. Figure 2B shows the Zr contents of rutile sorted by textural position: trapped in NI, included in MI-bearing garnet and in the matrix. All three rutile types display a high variability of Zr content, a common feature in high-grade rocks. Considering the highest Zr values as representative of the peak *T* (see Luvizotto and Zack, 2009), the *T* range between the production of melt and its subsequent entrapment in garnet is from >1000° to 930°C (Fig. 2B), indicating that the interpretation of MI as former UHT melts is robust.

GEOCHEMISTRY OF UHT MELTS

Only GI containing fresh glass have been analysed for major elements and H_2O. The melts are granitic, weakly peraluminous [ASI (molar Al/(Ca+Na+K)) = 0.95–1.12], sometimes peralkaline (Fig. 3A), typically ferroan (Fig. 3B), with high SiO_2 (76–78 wt.%) and K_2O + Na_2O (8.6–10.5 wt.%; Fig. 3C) and with K_2O/Na_2O from 2.5 to 7.5. They exhibit low maficity (FeO + MgO = 0.5–1.1 wt.%), Al_2O_3 (11–12.6 wt.%) and very low CaO (0.06–0.4 wt.%). All GI have low H_2O contents, usually <1.3 wt.% (measured by Raman; see Data Repository).

Trace elements measured in both NI and GI show that MI are rich in Cs (10–89 ppm), Rb (146–711 ppm) and Ga (20–51 ppm), but contain low Ba (225–890 ppm), Sr (7–48 ppm) and intermediate to low Zr (32–376 ppm; Fig 3D). Zr saturation temperatures (Crisp and Berry, 2022) of the melts vary from 712 to 931°C (see discussion below).

THE LINK BETWEEN ANATECTIC UHT MELTS AND A-TYPE GRANITES

Most A-type suites exhibit a large range in silica (55–78 wt.%) and products having ≥75 wt.% SiO_2 are considered subordinate (Frost and Frost, 2011). The investigated UHT MI all have SiO_2 ≥ 76 wt.%, but several of their geochemical features (e.g., ferroan character, ASI 0.95-1.1, high alkali and K/Na, Rb and Ga, low Al_2O_3, Ba, Sr, and H_2O) are typical of A-type granites (Fig. 3A-C). Indeed, in the classification diagrams from Whalen et al. (1987), MI plot in the field of A-type granites, together with other high-SiO_2 occurrences described in landmark papers on these rocks (Fig. 3C-D).

Zirconium > 200 ppm is considered diagnostic of many A-type granites, and attributed to the dissolution of zircon at HT-UHT conditions (Collins et al. 1982); yet most of our MI show lower Zr values (Fig. 3D). Such discrepancy can be due to the fact that, unlike predictions of equilibrium solubility models, zircon in rocks from Rundvågshetta also grew during prograde path, surviving UHT conditions (Durgalakshmi et al., 2021). Moreover, the fast garnet growth rates, necessary to trap MI, probably prevented melt-zircon equilibrium to be achieved, as documented in other MI studies (Acosta-Vigil et al., 2012). This complexity of anatexis mechanisms imposes caution when converting the Zr content of MI into magmatic *T* estimates.

The restricted, high-SiO_2 content of MI in this study finds analogies in occurrences of A-type granites dominated by felsic rocks: Topsails igneous terrane, Western Newfoundland (43% and 57% of analyzed rocks with 70–75 and 76–78 wt.% SiO_2, respectively; Whalen et al., 1987), Gabo (all with 72–75 wt.% SiO_2) and Mumbulla (all with 77–79 wt.% SiO_2) suites of southern Australia (Collins et al., 1982) and White Mountains suite (67% with 70–75 wt.% SiO_2, 16% >75 wt.% SiO_2; Eby, 1990). In the large dataset of Dubray et al. (2018) on ferroan granites from United States, 68% of the samples are >70 wt.% SiO_2, and some localities (e.g., Dells granite) are almost totally characterized by rocks with ≥73 wt.% SiO_2.

As the primary composition of most granites is modified by multiple processes including magma mixing/mingling and/or accumulation of early crystallized feldspars (e.g., Brown et al., 2016), we performed geochemical modelling considering the large-ion lithophile elements (Rb, Sr, and Ba) which are sensitive to these processes. Results show that the composition of less felsic (SiO_2 < 70 wt.%) A-type magmas – whose hybrid origin has been proposed (Smithies et al., 2011) – is well reproduced by mixing UHT MI and a mantle-derived component (Fig. 4A and B). Conversely, high-SiO_2 rocks (> 70 wt.%) do not show a clear trend toward the mafic component; rather, there is a partial overlap of MI with some A-type granites and most of compositional variability in the latter can be explained by accumulation of K-feldspar and plagioclase, starting from parental melts represented by UHT MI (Fig. 4A and B). Considering granitoids as crystal cumulates from which interstitial melt may be extracted to form high-SiO_2 volcanic rocks (Deering and Bachmann, 2010), it is not surprising that the predicted composition of evolved model melt is similar to A-type rhyolites. Accumulation of feldspars, as suggested by trace element modelling (Fig. 4A and B), can also extend the silica range to lower values (Fig. 4C). This reinforces the

view that the MI from this study can represent the primary melts of high-SiO_2, weakly peraluminous A-type granites.

IMPLICATIONS

A-type granites have not been considered to derive from melting of metasediments probably because most experiments of metapelites produced melts that are insufficiently ferroan and/or too strongly peraluminous (Fig. 3A and B; Gao et al., 2016). However, experiments have reproduced only closed systems behaviour, where the composition of UHT melts produced from fertile sources is the integrated mixture of the melts generated over a *T* interval >200 °C.

The pristine natural UHT melts investigated in this study, together with in-source context in which they occur, show instead that residual metasedimentary crust can produce melts representing high-SiO_2 end-members in the wider compositional spectrum of A-type igneous suites. Therefore, our findings are also consistent with a metasedimentary origin of A-type granites suggested on the basis of zircon, whole-rock and isotopic data (e.g., Huang et al., 2011; Zhang et al., 2022) and indicate that anatexis of metasediments should not only be correlated to S-type granite magmatism. Indeed, a weakly peraluminous character (ASI=1) is expected for melts with <1 wt.% H_2O, despite the strongly peraluminous source (Acosta Vigil et al., 2003).

Other MI studies (Cesare et al., 2015) of less residual metasedimentary sources report strongly peraluminous S-type granite compositions at *T* approaching UHT conditions (Cesare et al., 2015), whereas in this study a residual source produces melts akin to high-SiO_2 A-type granites. Hence, our results question the fertile-source model (Creaser et al., 1991; Frost and Frost, 2011). Rather, we argue that pre-conditioning of the crust (i.e., when a large amount of melt has previously been extracted and thermal buffering of melting reactions is less efficient; Vielzeuf et al., 1990) may be essential in the formation of A-type granites. This would allow the achievement of UHT conditions (with or without the mantle involvement), promoting further low-fraction melting of a residual protolith (12 vol.% melt at 1000 °C; this study). The latter can have a metasedimentary origin (this study; Huang et al., 2011; Zhang et al., 2022) or an igneous one (Collins et al., 1982), resulting in the formation of S- and I-type melts during previous anatexis.

A-type granites are less voluminous than S- and I-types in the crust, and when present they often post-date them (Collins et al., 1982; 2021). This is consistent with the residual character of the crustal source and with the fact that UHT conditions in the crust are subordinate. Nonetheless,

considering the size of exposed UHT terranes (largest being >10000 km^2; Qi et al., 2022), the inferred thickness of crust that could undergo UHT melting (ca. 15 km, Zhang et al., 2022) and the often long-lived duration of UHT metamorphism (Harley, 2016), it is possible that even small degrees of melting can generate significant volumes of A-type granites. For example, the low-degree (10%) melting of a UHT terrane of 10000 km^2 by 10 km thickness could feed a 1 km-thick intrusion of A-type granite covering the entire terrane. This conceptual model is supported by the spatial and temporal association of UHT metamorphism and A-type granite magmatism throughout eastern Gondwana terranes in Antarctica, Madagascar, and southern India (Jacobs et al., 2008; Sato et al., 2010; Tsunogae and Santosh, 2010). These findings call for a revaluation of the commonly accepted view that only S-type granites image the geodynamic evolution of the high-grade metasedimentary crust.

ACKNOWLEDGMENTS

This study benefited from several sources of funding: PNRA2018_103 to BBC., Cariparo Makearth and Prin 2017ZE49E7 to BC and BART_SID19_01 to OB. BBC is thankful to Martin Hand for sharing his knowledge on UHT metamorphism. Editorial handling from Marc Norman and constructive reviews from B. Bonin, C.D. Frost and H. Huang improved the manuscript.

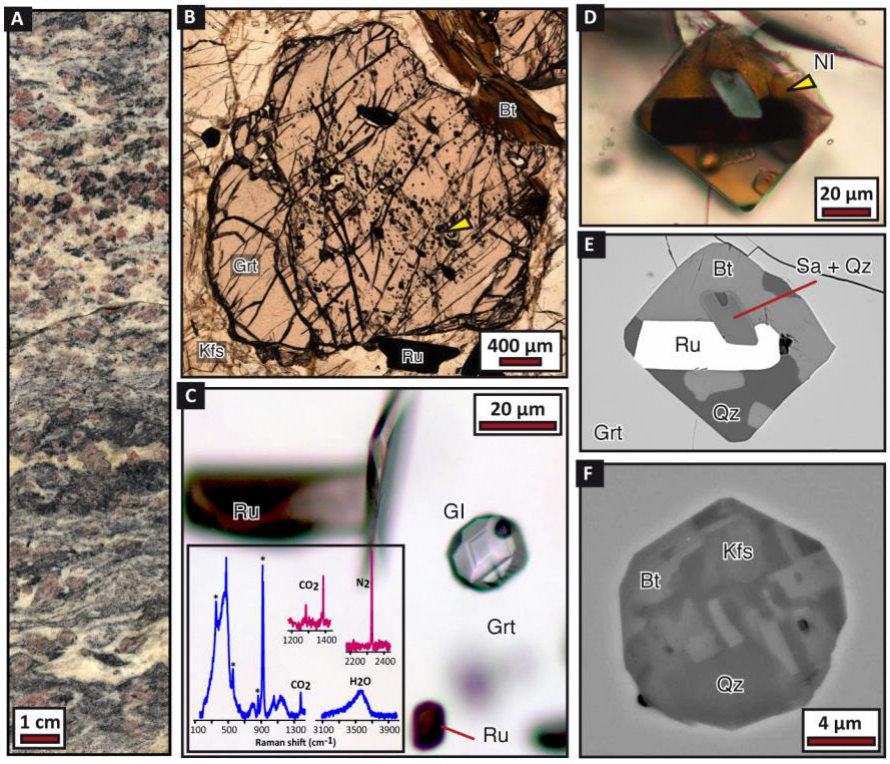

Figure 1. A) Macroscopic view of the metapelitic UHT granulite from Rundvågshetta. B) Garnet (Grt) with abundant inclusions in its core, C) Negative crystal shaped glassy melt inclusion (GI) associated to rutile (Ru) in Grt. Inset: Raman spectra (cm^{-1}) of the glass (blue) and bubble (pink). D) Nanogranitoid (NI) containing trapped Ru + sapphirine (Sa) + quartz (Qz). E) BSE image of the NI in (D). F) BSE image of a NI containing K-feldspar (Kfs), biotite (Bt) and Qz.

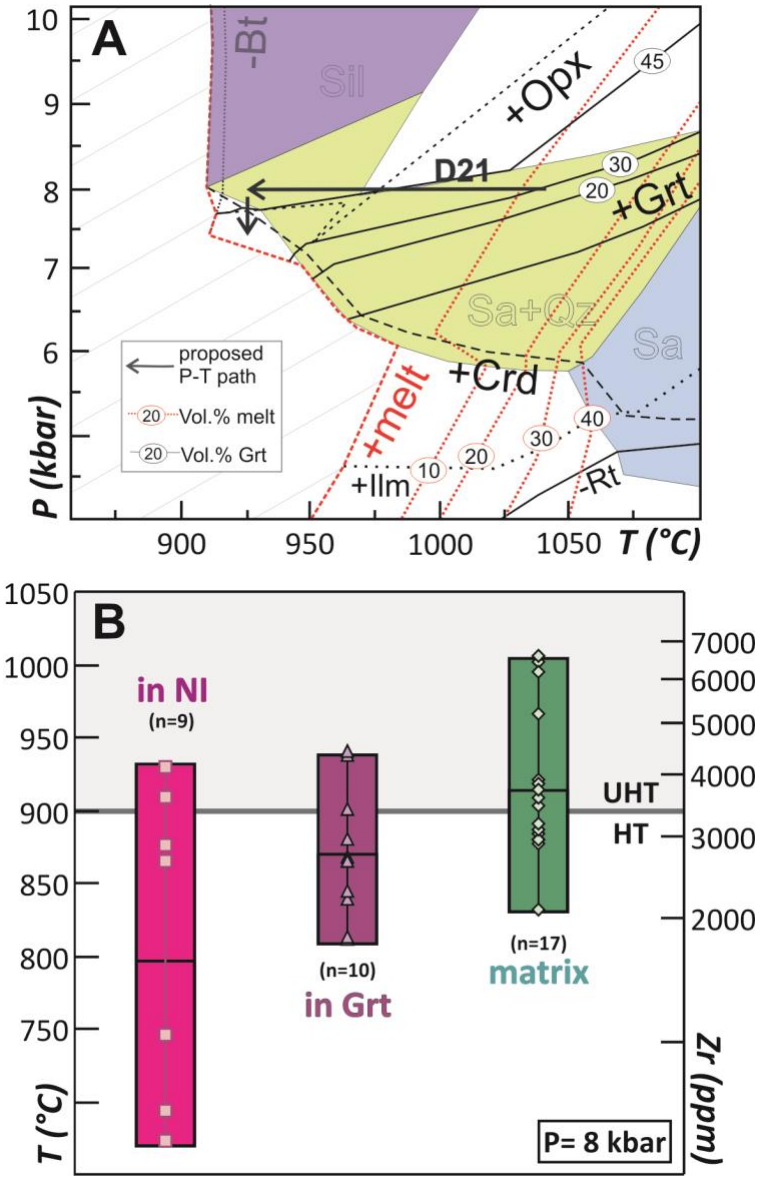

Figure 2. A) *P–T* phase diagram showing stability fields of key minerals, with garnet and melt modes. D21: path from Durgalakshmi et al. (2021). B) T (°C) and Zr contents (ppm) of rutile in nanogranitoid (in NI), in garnet (in Grt) and in the matrix. Temperatures calculated at 8 kbar (Table DR4). Horizontal bars are median, and colored boxes highlight the whole variability in each microstructural position. T>900°C (UHT metamorphism) is highlighted in grey.

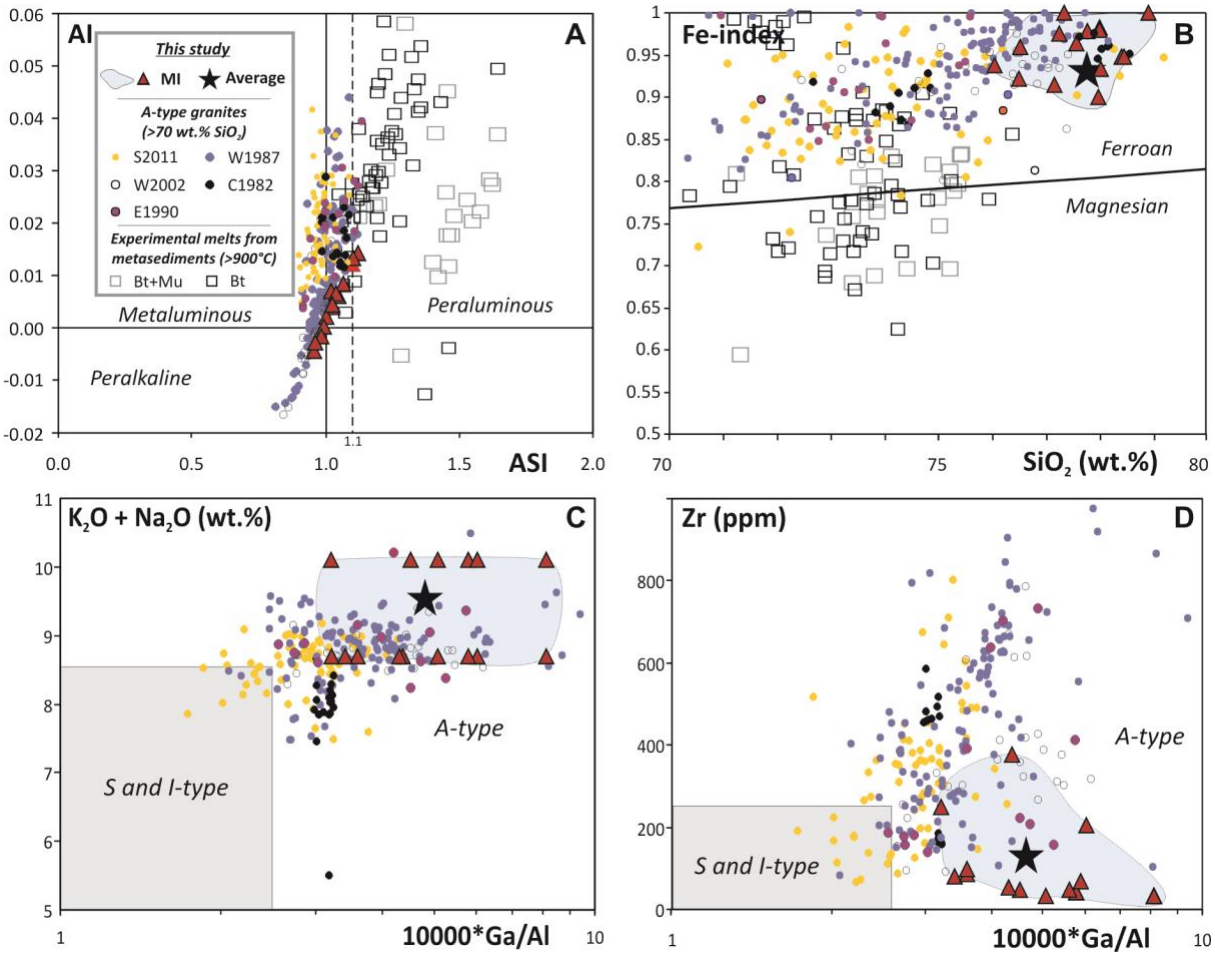

Figure 3. Geochemical features of UHT melts from this study compared with A-type granites (SiO_2 > 70 wt%) and UHT experimental melts from metasedimentary protoliths (Gao et al., 2016). A) Plot of alkalinity index (AI = molar Al-Na+K) vs. aluminium saturation index (ASI), and B) Fe-index ($FeO_t/FeO_t + MgO$) vs. SiO_2 (from Frost and Frost, 2011). C and D) Classification diagrams from Whalen et al. (1987). Maxima and minima of $K_2O + Na_2O$ in (C) are used for different Ga/Al ratios, since only MI below garnet surface were analysed for trace elements. Data from the literature: C1982 (Collins et al., 1982); W1987 (Whalen et al., 1987); E1990 (Eby, 1990); W2002 (Wu et al., 2002); S2011 (Smithies et al., 2011).

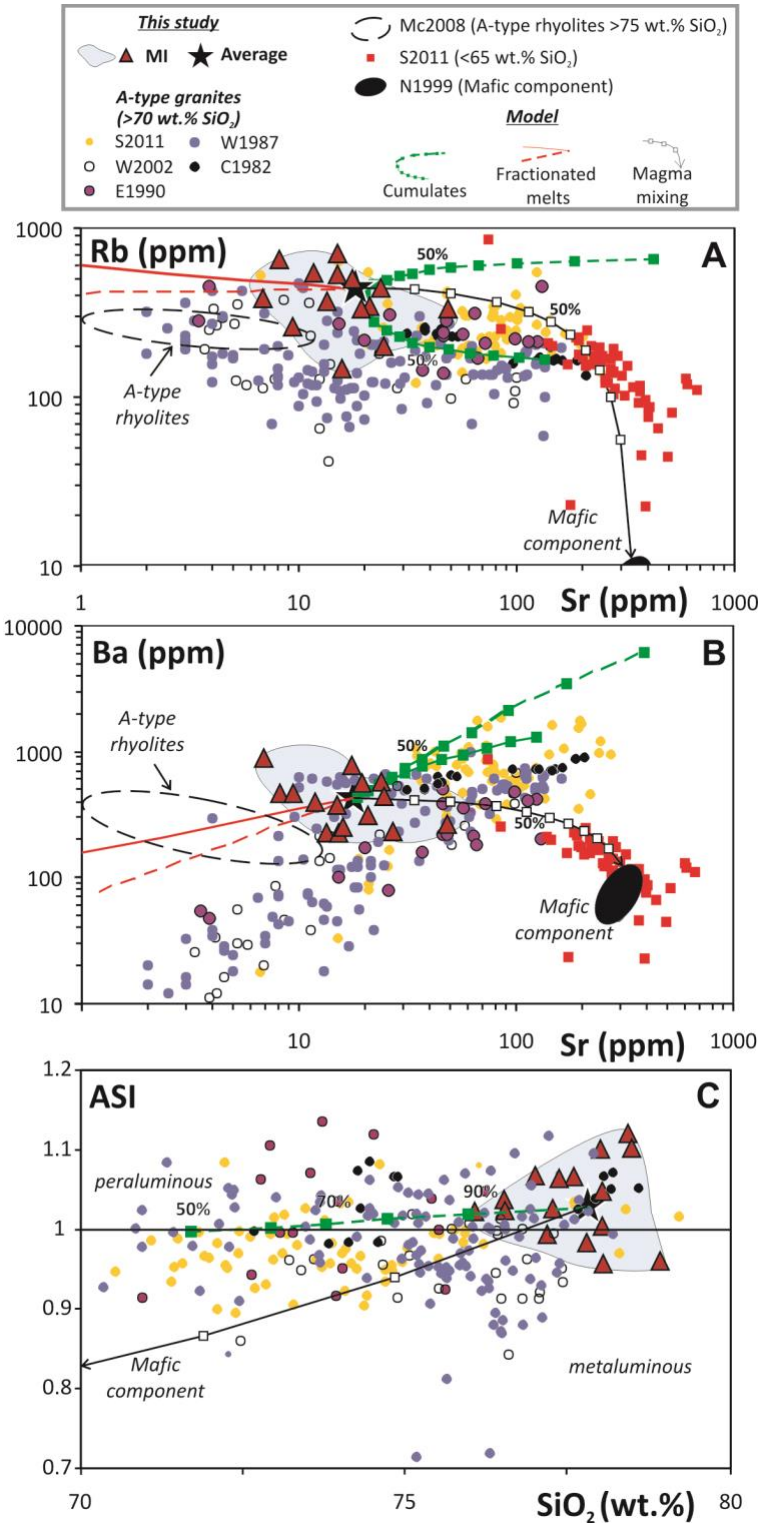

Figure 4. Plots of A) Sr vs. Rb, B) Sr vs. Ba and C) SiO_2 vs. ASI for UHT MI and A-type granites. Rayleigh fractional crystallization models for trace elements use the average MI as starting composition and track the evolution of cumulate and residual melt, considering different partition coefficients and crystallization of 70% Kfs and 30% Pl (see Data Repository). A mixing model is also reported. Squares (steps of 10%) indicate the fraction of melt remaining or

the amount of mafic magma in the model. A-type granites are described in Fig. 3, A-type rhyolites >75 wt.% SiO_2 from Mc2008 (McCurry et al., 2008), intermediate to mafic lithotypes (<65 wt.% SiO_2, S2011) from Smithies et al. (2011) and mafic component N1999 from Naumann and Geist (1999).

REFERENCES

Acosta-Vigil, A., London, D., Morgan, G.B., and Dewers, T.A., 2003, Solubility of excess alumina in hydrous granitic melts in equilibrium with peraluminous minerals at 700–800 C and 200 MPa, and applications of the aluminum saturation index: Contributions to Mineralogy and Petrology, v. 146, p. 100–119.

Acosta-Vigil, A., Buick, I., Cesare, B., London, D., Morgan, G.B., 2012, The extent of equilibration between melt and residuum during regional anatexis and its implications for differentiation of the continental crust: a study of partially melted metapelitic enclaves. Journal of Petrology, v. 53, p.1319-1356.

Bonin, B., 2007, A-type granites and related rocks: evolution of a concept, problems and prospects: Lithos, v. 97, p. 1–29.

Brown, C.R., Yakymchuk, C., Brown, M., Fanning, C.M., Korhonen, F.J., Piccoli, P.M., and Siddoway, C.S., 2016, From source to sink: petrogenesis of Cretaceous anatectic granites from the Fosdick migmatite–granite complex, West Antarctica: Journal of Petrology, v. 57, p. 1241–1278.

Cesare, B., Acosta-Vigil, A., Bartoli, O., and Ferrero, S., 2015, What can we learn from melt inclusions in migmatites and granulites?: Lithos, v. 239, p. 186–216.

Clark, C., Fitzsimons, I.C., Healy, D., and Harley, S.L., 2011, How does the continental crust get really hot?: Elements, v. 7, p. 235–240.

Clemens, J.D., Holloway, J.R., and White, A.J.R., 1986, Origin of an A-type granite; experimental constraints: American Mineralogist, v. 71, p. 317–324.

Collins, W.J., Beams, S.D., White, A.J.R., and Chappell, B.W., 1982, Nature and origin of A-type granites with particular reference to southeastern Australia. Contributions to Mineralogy and Petrology, v. 80, p. 189–200.

Collins, W.J., Murphy, J.B., Blereau, E., and Huang, H.Q., 2021, Water availability controls crustal melting temperatures: Lithos, v. 402, 106351.

Creaser, R.A., Price, R.C., and Wormald, R.J., 1991, A-type granites revisited: assessment of a residual-source model: Geology, v. 19, p. 163–166.

Crisp, L. J., and Berry, A. J., 2022. A new model for zircon saturation in silicate melts. Contributions to Mineralogy and Petrology, v. 177, p. 71.

Deering, C.D., and Bachmann, O., 2010, Trace element indicators of crystal accumulation in silicic igneous rocks: Earth and Planetary Science Letters, v. 297, p. 324–331.

Dubray, E.A., Holm-Denoma, C.S., Lund, K., Premo, W.R., 2018. Review of the Geo-chemistry and Metallogeny of Approximately 1.4 Ga Granitoid Intrusions of the Conterminous United States. U.S. Geological Survey Scientif. Invest. Report 2017-5111

Durgalakshmi, I., Sajeev, K., Williams, I.S., Reddy, D.H., Satish-Kumar, M., Jöns, N., Sanjeewa, P., Vinod, S., and George, P.M., 2021, The timing, duration and conditions of UHT metamorphism in remnants of the former eastern Gondwana: Journal of Petrology, v. 62, egab068. https://doi.org/10.1093/petrology/egab068

Eby, G.N., 1990, The A-type granitoids: a review of their occurrence and chemical characteristics and speculations on their petrogenesis: Lithos, v. 26, p. 115–134.

285 Eby, G.N., 1992, Chemical subdivision of the A-type granitoids: petrogenetic and tectonic
286 implications: Geology, v. 20, p. 641–644.
287 Frost, C.D., and Frost, B.R., 2011, On ferroan (A-type) granitoids: their compositional variability
288 and modes of origin: Journal of Petrology, v. 52, p. 39–53.
289 Gao, P., Zheng, Y. F., and Zhao, Z. F., 2016, Experimental melts from crustal rocks: a
290 lithochemical constraint on granite petrogenesis. Lithos, v.266, p. 133-157.
291 Harley, S.L., 2016, A matter of time: The importance of duration of UHT metamorphism.
292 Journal of Mineralogical and Petrological Sciences, v. 111, p. 50-72.
293 Huang, H.Q., Li, X.H., Li, W.X., and Li, Z.X., 2011, Formation of high $\delta^{18}O$ fayalite-bearing A-
294 type granite by high-temperature melting of granulitic metasedimentary rocks, southern
295 China: Geology, v. 39, p. 903–906.
296 Jacobs, J., Bingen, B., Thomas, R. J., Bauer, W., Wingate, M. T., and Feitio, P., 2008. Early
297 Palaeozoic orogenic collapse and voluminous late-tectonic magmatism in Dronning Maud
298 Land and Mozambique: insights into the partially delaminated orogenic root of the East
299 African–Antarctic Orogen?. Geological Society, London, Special Publications, v.308, p. 69-
300 90.
301 Kelsey, D.E., and Hand, M., 2015, On ultrahigh temperature crustal metamorphism: phase
302 equilibria, trace element thermometry, bulk composition, heat sources, timescales and
303 tectonic settings. Geoscience Frontiers, v. 6, p. 311–356.
304 King, P.L., White, A.J.R., Chappell, B.W., and Allen, C.M., 1997, Characterization and origin of
305 aluminous A-type granites from the Lachlan Fold Belt, southeastern Australia: Journal of
306 Petrology, v. 38, p. 371–391.

307 Luvizotto, G. L., Zack, T., 2009, Nb and Zr behavior in rutile during high-grade metamorphism
308 and retrogression: an example from the Ivrea–Verbano Zone. Chemical Geology, v. 261,
309 303-317.
310 McCurry, M., Hayden, K.P., Morse, L.H., and Mertzman, S., 2008, Genesis of post-hotspot, A-
311 type rhyolite of the Eastern Snake River Plain volcanic field by extreme fractional
312 crystallization of olivine tholeiite: Bulletin of Volcanology, v. 70, p. 361–383.
313 Naumann, T.R., and Geist, D.J., 1999, Generation of alkalic basalt by crystal fractionation of
314 tholeiitic magma: Geology, v. 27, p. 423–426.
315 Patiño Douce, A.E., 1997, Generation of metaluminous A-type granites by low-pressure melting
316 of calc-alkaline granitoids: Geology, v. 25, p. 743–746.
317 Qi, Y., Kohn, M. J., Huang, G., Zheng, Y., Jiao, S., Guo, J., 2022. Thermal regime of the lower
318 crust in the eastern Khondalite Belt, North China Craton, constrained by Zr-in-rutile
319 thermometry mapping. Precambrian Research, v. 377, 106720.
320 Sato, K., Santosh, M., Tsunogae, T., Kon, Y., Yamamoto, S., Hirata, T., 2010. Laser ablation
321 ICP mass spectrometry for zircon U–Pb geochronology of ultrahigh-temperature gneisses
322 and A-type granites from the Achankovil Suture Zone, southern India. Journal of
323 Geodynamics, v.50, p. 286-299.
324 Smithies, R.H., Howard, H.M., Evins, P.M., Kirkland, C.L., Kelsey, D.E., Hand, M., Wingate,
325 M.T.D., Collins, A.S., and Belousova, E., 2011, High-temperature granite magmatism,
326 crust–mantle interaction and the Mesoproterozoic intracontinental evolution of the
327 Musgrave Province, Central Australia: Journal of Petrology, v. 52, p. 931–958.
328 Tsunogae, T., and Santosh, M., 2010, Ultrahigh-temperature metamorphism and decompression
329 history of sapphirine granulites from Rajapalaiyam, southern India: implications for the

formation of hot orogens during Gondwana assembly. Geological Magazine, v. 147, p. 42-58.

Vielzeuf, D., Clemens, J. D., Pin, C., and Moinet, E., 1990, Granites, granulites, and crustal differentiation. In Granulites and crustal evolution (pp. 59-85). Springer, Dordrecht.

Whalen, J.B., Currie, K.L., and Chappell, B.W., 1987, A-type granites: geochemical characteristics, discrimination and petrogenesis. Contributions to mineralogy and petrology, v. 95, p. 407-419.

Wu, F. Y., Sun, D. Y., Li, H., Jahn, B. M., and Wilde, S., 2002, A-type granites in northeastern China: age and geochemical constraints on their petrogenesis. Chemical Geology, v. 187, p. 143-173.

Zhang, X. Z., Wang, Q., Wyman, D., Kerr, A. C., Dan, W., Qi, Y., 2022, Tibetan Plateau insights into> 1100° C crustal melting in the Quaternary. Geology.